



## Bending Nematic Liquid Crystal Membranes with Phospholipids

Journal:	<i>Soft Matter</i>
Manuscript ID	SM-ART-06-2018-001193.R1
Article Type:	Paper
Date Submitted by the Author:	17-Jul-2018
Complete List of Authors:	<p>Cumberland, Jenieve; Kent State University, Chemical Physics          Lopatkina, Tetiana; Kent State University, Chemical Physics          Murachver, Matthew; Kent State University, Chemical Physics          Popov, Piotr; Kent State University, Chemical Physics          Kenderesi, Viktor; Magyar Tudomanyos Akademia Wigner Fizikai          Kutatokozpont          Buka, Ágnes; Institute for Solid State Physics and Optics, Wigner Research          Centre for Physics, Hungarian Academy of Sciences,          Mann, Elizabeth; Kent State University, Physics          Jakli, Antal; Kent State Univ, Liquid Crystal Institute</p>

## Bending Nematic Liquid Crystal Membranes with Phospholipids

Jenieve Cumberland<sup>a</sup>, Tetiana Lopatkina<sup>a</sup>, Matthew Murachver<sup>a</sup>, Piotr Popov<sup>b</sup>, Viktor Kenderesi<sup>c</sup>, Ágnes Buka<sup>c</sup>, Elizabeth Mann<sup>d</sup> and Antal Jákli<sup>a,c,d</sup>

<sup>a</sup> *Chemical Physics Interdisciplinary Program and Liquid Crystal Institute, Kent State University, Kent, OH, 44242 USA*

<sup>b</sup> *RavenWindow, Inc., Denver CO, 80207, USA*

<sup>c</sup> *Institute for Solid State Physics and Optics, Wigner Research Centre for Physics of the Hungarian Academy of Sciences, 1525 Budapest, Hungary*

<sup>d</sup> *Department of Physics, Kent State University, Kent, OH, 44242, USA*

*\*Corresponding author: [ajakli@kent.edu](mailto:ajakli@kent.edu)*

### Abstract

The interactions of phospholipids with liquid crystals have formed the basis of attractive biosensor technologies, but many questions remain concerning the basic physics and chemistry of these interactions. Phospholipids such as 1,2-dilauroyl-sn-glycero-3-phosphocholine (DLPC), at sufficiently high ( $\sim 1\mu\text{M}$ ) concentrations, and/or sufficiently long times, turn the liquid crystal director perpendicular to the LC/water interface. If the other side of the LC film is in contact with a surface that prefers perpendicular alignment, the LC film appears completely dark between crossed polarizers. Recently, however, Popov et al. (J. Mater. Chem. B, 2017, 5, 5061) noted that at even higher ( $\sim 10\mu\text{M}$ ) DLPC concentrations, the liquid crystal texture brightens again between crossed polarizers. To explain this surprising observation, it was suggested that the LC interface might bend. In this paper we show by optical surface profiler measurements that indeed the interface of the LC film of 4-cyano-4'-octylbiphenyl (8CB) suspended in a transmission electron microscopy (TEM) grid with openings of  $\sim 0.5\mu\text{m}$  in diameter bends towards the lipid-coated interface. We demonstrate that where the bending occurs, the bent interface exhibits extreme sensitivity to air pressure variations, producing an optical response with acoustic stimulation. Finally, we suggest a physical mechanism for this astonishing result.

## Introduction

Thermotropic liquid crystals are generally hydrophobic (oily) and do not mix with water or other hydrophilic materials, such as glycerol. Instead, they form a molecularly-thin interface with aqueous media.<sup>1-6</sup> The alignment of the LC at interfaces determines the bulk alignment of the liquid crystal molecules, which is thus extremely sensitive to the aqueous medium. This sensitivity to a molecularly-thin area of contact is the principle behind thermotropic liquid crystal-based biosensors, as proposed first by Abbott et al.<sup>7</sup> and reviewed recently in several excellent articles<sup>8-16</sup> Common LC molecules, such as 5CB and 8CB (cyano-biphenyl core and alkyl tail with 5 and 8 carbons, respectively), are oriented at random directions almost parallel to hydrophilic surfaces such as water.<sup>6</sup> However, if the hydrophilic medium contains surfactants or lipids, these diffuse to the LC interface and change the alignment to normal to the interface (homeotropic).<sup>12,14,17-21</sup> In typical LC biosensors, the other interface of the thin (5-50 $\mu$ m) LC film is in contact with a material that promotes homeotropic alignment, such as suitably-treated solid substrates<sup>7</sup> or air<sup>22</sup>. This arrangement leads to a birefringent hybrid alignment, which appears bright between crossed linear or left and right circular polarizers, at zero surfactant concentration. However, when the surfactant realigns the director on the aqueous interface to homeotropic, the entire liquid crystal film assumes the homeotropic alignment, which is dark between crossed or left/right circular polarizers when illuminated with light at normal incidence (i.e., in microscopes). In all these biosensors, the effect of the analytes in the aqueous media is restricted to realignment that leaves the shape of the interface unchanged: the effect is purely optical.

In a recent experiment involving 1,2-dilauroyl-sn-glycero-3-phosphocholine (DLPC; Figure 1(b)) and a well-known commercially-available liquid crystal, 4-cyano-4'-ocylbiphenyl (8CB, Figure 1(a)), an interesting optical effect was reported.<sup>16</sup> The 8CB was suspended in a 20 $\mu$ m thick transmission electron microscopy (TEM) grid with air in one side and DLPC dispersed in deionized water well above the critical aggregation concentration on the other side. Upon increasing the DLPC concentration, first the director at the LC/water interface became perpendicular to the substrate, which was manifested itself by a completely dark picture between crossed polarizers. However when the concentration was increased further, to above 10  $\mu$ M (or after a wait of several minutes), the picture brightened again [see Figure 1(c) and (d)]. In the

absence of a physical mechanism for high concentrations of lipid to cause a varying tilt of the director with respect to the vertical film normal, it was suggested that this brightening was due to bending of the film. This hypothesis is compatible with the dark spot in the center between both circular and crossed linear polarizers as seen in *Figure 1(c)* and (d), respectively, resembling a conoscopic image of homeotropic alignment in converging light. However, this hypothesis had not been experimentally tested and no quantitative measurements on the bending had been carried out.

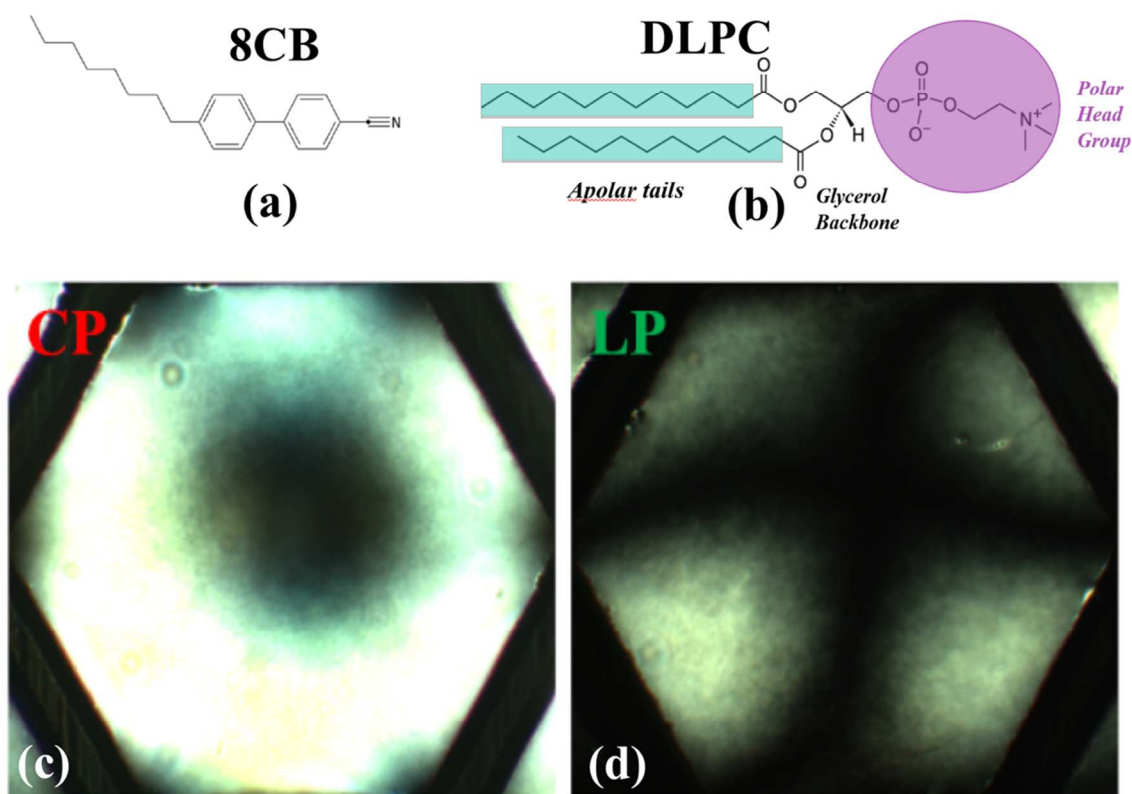


Figure 1. (a) Chemical structure of thermotropic 8CB liquid crystal. (b) Chemical structure of phospholipid DLPC and a common simplification for drawing a typical phospholipid. (c) A free standing thin film of 8CB in a 20 $\mu\text{m}$  thick transmission electron microscopy in contact with air on one side and a 10 mM solution of DLPC on the other, looking from below, viewed between circular polarizers. (d) The same viewed between linear polarizers. A hexagon edge is 250  $\mu\text{m}$  long.

In this article, we show by optical surface profiler measurements that 8CB films suspended in sub-millimeter size TEM grids indeed bend toward the lipid-coated interface. We also demonstrate that simultaneously with the bending, the LC film becomes extremely sensitive

to air pressure variations caused by sound. Finally, we suggest a reasonable physical mechanism that leads to these astonishing results.

## Experiments

For our experiment we used the same liquid crystal (8CB) and phospholipid (DLPC) as in the previous experiments by Popov et al.<sup>16</sup>, but with a slightly different sample holder (described below) that was compatible with the profiler geometry. Additionally, we replaced water with glycerol, because the water evaporated very quickly due to a dehumidifier required for the analyzing instrument. The experimental procedure follows:

- A dispersion of DLPC phospholipid, purchased from Avanti Polar Lipids, Inc., was prepared in a 1-dram glass vial with deionized water. First, 2.5 mg of lipid was added into the bottle followed by a small amount of chloroform. The solution was then placed into a vacuum oven for three hours. Once the chloroform completely evaporated, 4 ml of deionized water was added. The resulting dispersion of DLPC vesicles was held in a refrigerator at 5°C until needed. Since the dispersion is always in pure water or glycerol, the  $\text{pH} \sim 6$ ; DLPC is zwitterionic in that  $\text{pH}$  range.

- A rectangular glass container with a circular opening on one side was custom-made for this experiment. A glass capillary was inserted into the opening and one half of a nickel double TEM grid was horizontally suspended in air (see Figure 2(a)). Grids were purchased from Ted Pella, Inc., and were 20- $\mu\text{m}$  thick with a diameter of 3.05mm. The individual holes were hexagonal, with 250  $\mu\text{m}$  edge lengths. A rubber O-ring was glued to the container securing the glass capillary in a parallel position in preparation for microscopic observation, as well as to prevent solvent escape. One side of the TEM grid is placed inside the capillary and secured with a static friction force alone. The clearance of the 30 $\mu\text{m}$  capillaries fit the 20 $\mu\text{m}$  grid snug.

- 8CB was spread on one of the TEM grid halves to fill each cell evenly. Uniformity of the film thickness was tested by the uniformity of the color between left and right circular polarizers. Cells suspended in air assumed homeotropic alignment, as confirmed with Olympus BX60 Polarized Optical Microscope (POM).

2.2 ml of glycerol was then added into the container. The glycerol provided basically the same optical effect as water, as demonstrated in comparing Figures 1 and 2(b-d): hybrid

alignment at the air/glycerol interface [Figure 2(b)], homeotropic alignment with a 5  $\mu\text{M}$  DLPC concentration [Figure 2(c)], and light gray near away from the center at DLPC concentrations above 15  $\mu\text{M}$  [Figure 2(d), compared to Figure 1(d)]. As judged from the Michel-Lévy chart, the light gray appearance of the 20- $\mu\text{m}$  8CB film indicates an effective birefringence of  $\Delta n_{eff} \approx 0.005$ .

$$\Delta n_{eff} = \frac{n_{\perp} n_{\parallel}}{\sqrt{n_{\parallel}^2 \cos^2 \theta + n_{\perp}^2 \sin^2 \theta}} - n_{\perp},^{23}$$

where  $n_{\perp} \sim 1.53$  and  $n_{\parallel} \sim 1.71$  are the refractive indices perpendicular and parallel of the director of 8CB in the N phase far from the isotropic phase. From this the angle  $\theta$  that the director makes with respect to the vertical light can be estimated to be about 3-5 degrees.

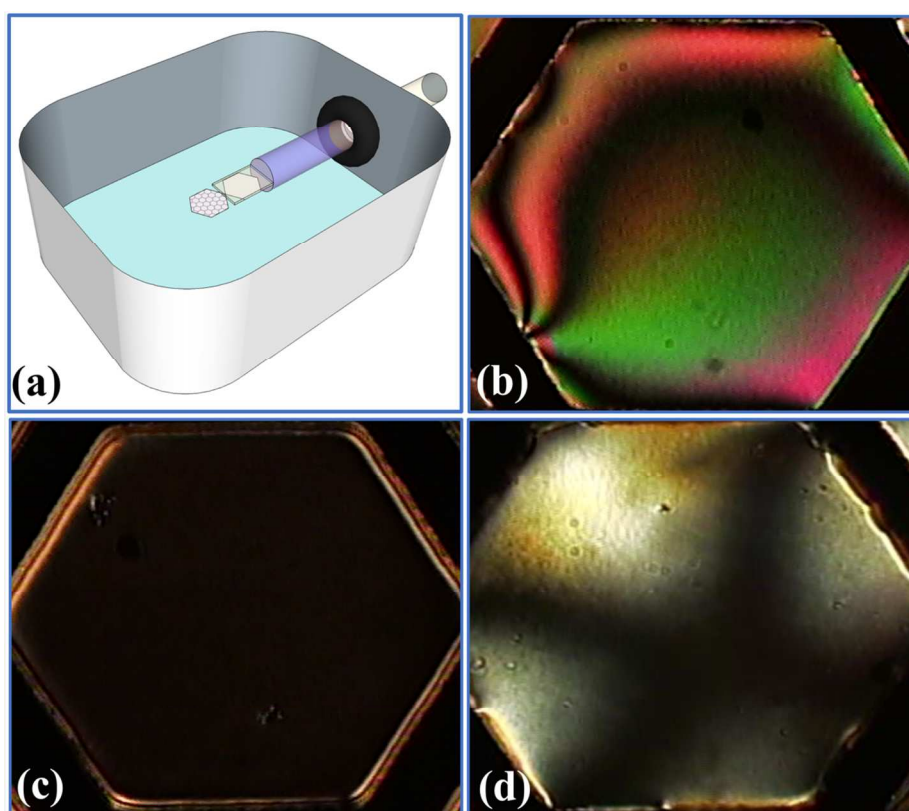


Figure 2: (a) Sample container and TEM Grid holder. (b-d) Alignment of 8CB in an individual hexagonal cell seen between crossed polarizers at 37°C. (b) Hybrid alignment at air/glycerol interfaces; (c) Homeotropic alignment at air/(glycerol+5 $\mu\text{M}$  DLPC); (d) Brightened texture (oblique alignment) at air/(glycerol+40 $\mu\text{M}$  DLPC). Edge length of the hexagons is  $a=250\mu\text{m}$ .

After verifying that DLPC produced the same effect in glycerol as in water, we repeated the procedures used with water. The sample was placed under the 3D optical profiler instrument Zygo (NewView™ 7100). The 3D profiler is utilizing interference effects of unpolarized light

between the upper LC/air interface and the objective of the profiler. Additionally, the nematic director of the 8CB is homeotropic (quasi-isotropic at the air interface), and the deviation of the director from vertical is less than 3 degrees even in the most bent case, so any artifact due to optical anisotropy can be disregarded. Profiles were recorded for the configurations air/air, air/glycerol and air/(glycerol+DLPC) adding DLPC solution in multiples of 20  $\mu\text{L}$  ( $\sim 17 \mu\text{M}$  in the final glycerol solution), up to a maximum of 100  $\mu\text{L}$  ( $\sim 83 \mu\text{M}$ ).

## Results

Images of selected 3D profiles are shown in Figure 3. One can see that the top surface of the 8CB film is flat when the LC is between airs at both sides. When pure glycerol is added until it reached the grid, the surface appears to bulge slightly upward. Once DLPC is added at  $17 \mu\text{M}$ , the film bends downward with increasing depth at increasing DLPC concentration. Examples at  $66 \mu\text{M}$  and  $83 \mu\text{M}$  DLPC concentrations are shown as the bottom two images of Figure 3.

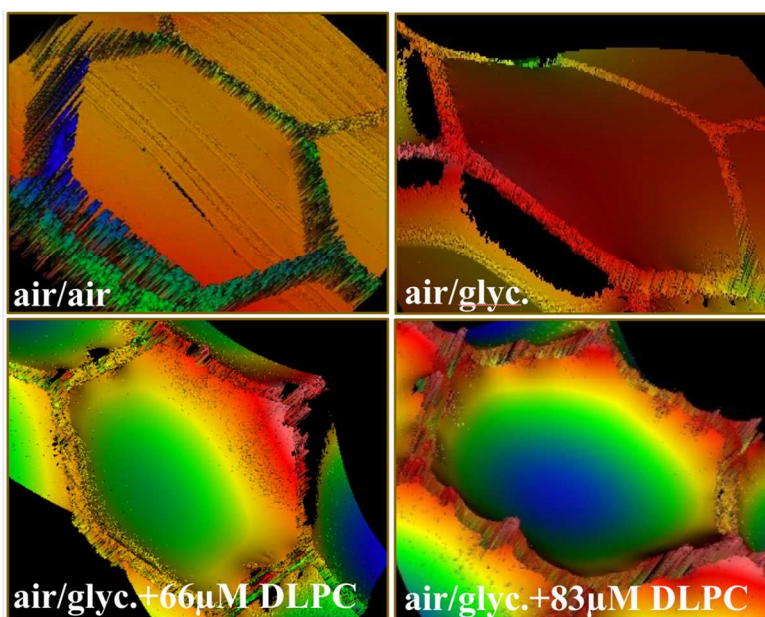


Figure 3: 3D profiles of  $20 \mu\text{m}$  8CB films suspended in  $290 \mu\text{m}$  side length hexagonal grids with different boundary conditions indicated in the individual images. An air-side of the grid is pointing to the top-right. In the presence of the lipid in the glycerol, the film is bent away from the air in the grid center.

2D profiles, measured along the largest distance between two apexes for the film at air/air, air/glycerol, air/(glycerol+DLPC at concentrations 17, 33, 66 and 83 $\mu\text{M}$ ) are shown in Figure 3. All profiles could be equally well fitted either by quadratic ( $y = q \cdot x^2$ ) or by catenary ( $y = a \cdot \cosh(x/a)$ ) functions. The LC membrane between air and air surfaces is basically horizontal ( $q=0$  for quadratic fitting). The film between air (top) and glycerol (bottom) is bent upward with a quadratic fit coefficient of  $q=-2.5 \times 10^{-5} \mu\text{m}^{-1}$ . The bulging at the air/glycerol interface at zero DLPC concentration is accidental and depends on the quantity of the original glycerol used. The bulging what we showed in the experimental series in Figure 4 was due to initial glycerol level that slightly passed the level of the grid. As we add DLPC the bulging changes sign and somewhere between 0 and 17  $\mu\text{M}$  the curvature becomes positive ( $q>0$ ). The quadratic coefficient is increasing with the DLPC concentration from  $6.6 \times 10^{-5}$  at 17 $\mu\text{M}$  to  $14 \times 10^{-5} \mu\text{M}$  at 83 $\mu\text{M}$ . As we added the DLPC in 17 $\mu\text{M}$  increments, we monitored the time variation of the POM images as the concentration increased gradually at the grid area. Every time it took about 5 minutes until the brightening saturated. During this period, the light intensity increased gradually without any jump. The 3D profiles were always measured more than 10 minutes after the DLPC was added, so they show saturated values.

The observed profiles are similar to those of chains and ropes sagging under their own weight when suspended between two points, or mechanically-fastened roofing membranes ballooning under wind-induced external pressure.<sup>24</sup> For circular flexible membranes, the maximum deflection  $h$  is related to the pressure difference  $\Delta P$ , radius of the membrane  $a$ , elastic modulus  $E$ , and thickness  $d$  as  $h \approx a \cdot 0.72(1 - \nu^2)^{1/3} \cdot (a \cdot \Delta P / E \cdot d)^{1/3}$ , where  $\nu$  is the Poisson ratio.<sup>24</sup> The LC membrane is incompressible, i.e.,  $\nu=0.5$  and  $E \cdot d = \gamma$ , where  $\gamma$  is the total surface tension of the *LC/air* and *LC/(glycerol+DLPC)* surfaces, which can be approximated as  $2.5 \cdot 10^{-2}$  and  $1.0 \cdot 10^{-2}$  N/m, respectively.<sup>25</sup> Approximating our hexagons with a circle of radius  $a=250 \mu\text{m}$ , the pressure difference is estimated to be  $3 \cdot 10^{-3}$  Pa ( $\sim 40$  dB) for  $h=4.5 \mu\text{m}$ , as seen with a 17  $\mu\text{M}$  DLPC concentration (*see* Figure 3). This is in the order of the sound pressure of normal conversation. However, since the deflection is proportional to the 1/3 power of the pressure difference, one can see that  $\Delta P=5 \cdot 10^{-5}$  Pa ( $\sim 9$  dB), which is the sound pressure of a calm breathing, can change the deflection by 1  $\mu\text{m}$ . Indeed, we found that in the deflected state, the birefringence of the LC membrane is very sensitive to even low voices. The



variation of color in rhythm to music coming from a smart phone is illustrated in the video in the Supporting Information. Such a small deflection does not cause an observable birefringence change when the LC membrane is not deflected ( $\theta_0=0$ ), since the effective birefringence at very small  $\Delta\theta$  depends on the square of  $\Delta\theta$ , whereas in the deflected state, the leading dependence is a linear function of  $\Delta\theta$  ( $\sim 2\theta_0\Delta\theta$ ).

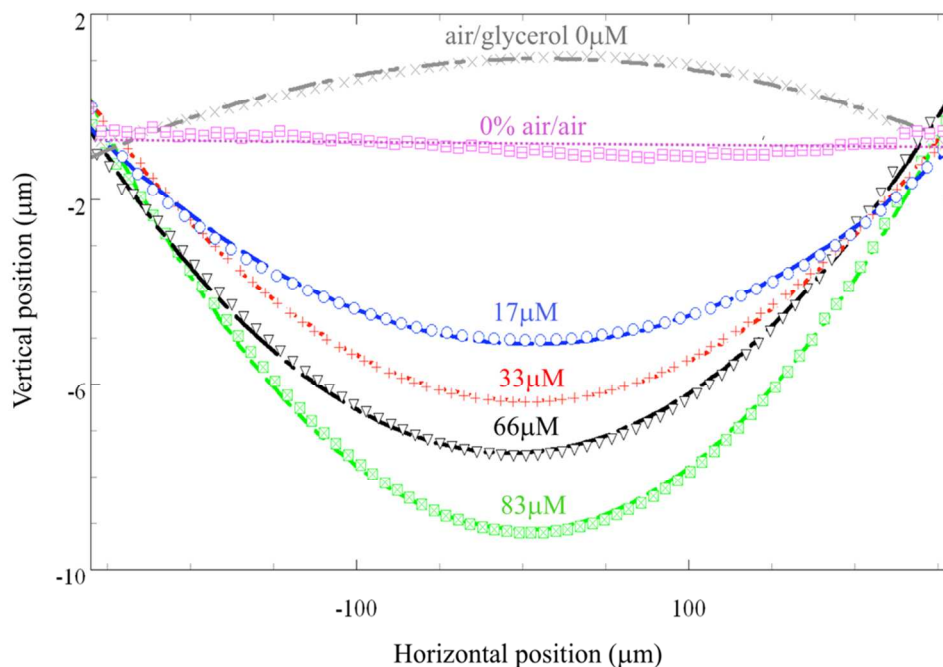


Figure 4: 2D profiles of 20- $\mu\text{m}$  thick 8CB films, measured from the center of one edge of a grid hexagon to the center of the opposite, parallel edge, going through the largest deflection of the film, with the film at the air/air, air/glycerol and air/(glycerol+DLP with 17, 33, 66 and 83 $\mu\text{M}$  concentrations) interfaces. Dotted lines are best fits using quadratic functions.

Importantly, the isotropic to nematic to smectic transition temperatures do not measurably changed upon the addition of the DLPC, which excludes the possibility that a significant portion of the amphiphile is absorbed into the 8CB film<sup>26</sup>. Finally we note that we have observed the radial brightness only with zwitterionic phospholipids, such as DLPC, DPPC and DOPE, which have double chains, and not for the anionic surfactant Sodium Dodecyl Sulfate (SDS) (that has only one chain) under similar experimental conditions.

## Discussion

The critical aggregate concentration (CAC) of DLPC in water is 100 nM,<sup>27</sup> so above this concentration DLPC molecules form more-or-less stable vesicles in aqueous solutions.<sup>28</sup> The concentrations of DLPC in this study are all over 1  $\mu\text{M}$ . Assuming that the CAC of DLPC is of the same order of magnitude in glycerol<sup>29</sup> as in water, most of the bulk DLPC molecules should be aggregated into vesicles. As these incoming vesicles interact with one another near the LC interface, they undergo shape transformations that induce topological changes such as vesicle rupturing<sup>30</sup>. After the vesicles open, the hydrophobic tails of the amphiphile are exposed to the hydrophobic tail of the LC molecules, and are favored by the free energy to adsorb to the LC interface. The hydrocarbon tail penetrates into the LC film and the hydrophilic phosphocholine headgroup faces the water or glycerol medium, Figure 5(a). As more amphiphile is added into the aqueous solution, the planar alignment gradually switches to homeotropic through the growing number and area of homeotropic patches.

Importantly, such a process can induce uniform homeotropic alignment even when the surface density of the DLPC is only slightly larger than the surface density of the glycerol molecules. This is because the uniform homeotropic alignment of the liquid crystal has lower energy per area than of the hybrid one by  $w=K/D$ , where  $K\sim 10$  pN is the Frank elastic constant and  $D=20\mu\text{m}$  is the thickness of the LC film. Since at the stage when the homeotropic alignment is completed the DLPC molecules are not tightly packed at the interface, there should be room for more DLPC molecules even after homeotropic alignment is complete. DLPC in vesicles is approximately cylindrically shaped: the occupied shape of flexible tails can be approximated as cylinders with length  $l_t$  area  $A_t$ , which is comparable to that of the optimal surface area  $A_h$  of the headgroup, promoting a flat interface.<sup>31</sup> Since for cylinders the occupied volume of the tails is  $V_t = A_t l_t$ , the surfactant packing parameter  $N_s = V_t/(A_h l_t)$  used to predict the shapes and sizes of micelles<sup>32</sup> and emulsions is very close to 1 ( $N_s\sim 1$ ). The interfacial region for this system, which includes both DLPC and 8CB, is complex, but when the DLPC is not tightly packed at the interface, we expect similar behavior, as shown in Figure 5(a).

Further increasing the density of the DLPC molecules at the LC interface, the surface pressure  $\pi=\gamma_0-\gamma$  increases, i.e., the LC/glycerol interfacial tension decreases from the original  $\gamma_0$  to  $\gamma$ , making the increase of the surface area by bending energetically less expensive. At the same

time, the increased surface pressure will push the fluctuating flexible tails to a more confined geometry, where they occupy less volume. However, the effective area of the head group  $A_h$  cannot be proportionally decreased, because the phosphocholine headgroup is zwitterionic, and neighboring charges or dipole moments repel each other when they are bound to a surface. The effective shape therefore can be approximated by a truncated cone with  $N_s < 1$ , and with a preference to aggregate into curved surfaces<sup>33–35</sup>. The bending effect of this reduced surfactant packing parameter is qualitatively illustrated in Figure 5(b). Note that such a bent surface means larger surface area, which can allocate more DLPC molecules, thus leading to a free energy decrease of the system.

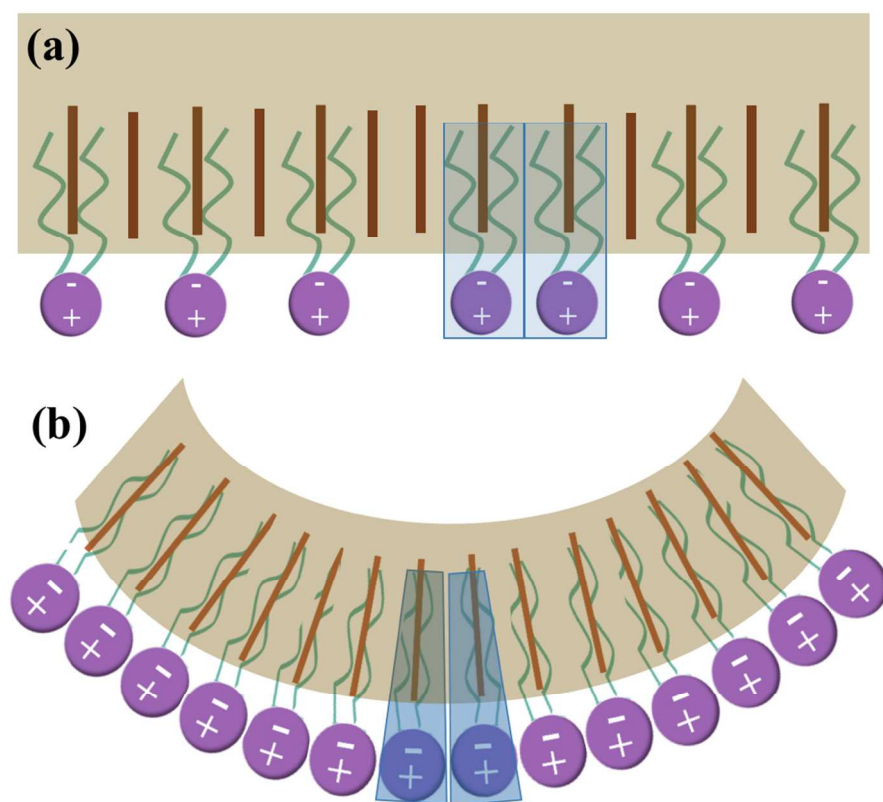


Figure 5: Illustration of the packing mechanism leading to the bending of the liquid crystal film covered by DLPC monolayer in the glycerol interface. The head purple circles indicate the effective headgroup size, including electrostatic repulsion between the charges and dipole moments. (a) At low and moderate DLPC surface density the area occupied by the alkyl tails is comparable to that of the optimal surface area of the headgroup ( $N_s \sim 1$ ), promoting flat interface. (b) At high DLPC surface density, the tails become less floppy and occupy smaller surface areas, whereas the zwitterionic head groups cannot get closer due to electrostatic repulsion between neighboring charges or dipole moments. This results in an effective bending of the liquid crystal film.

The change in packing parameter away from 1 implied by our measurements is very small, because the local curvature radii of the LC film are much larger than of the thickness of the lipid monolayer.

To test this model, we have added table salt ( $\text{NaCl}$ ) to the glycerol. The salt screens out the range of electrostatic interaction of the head group. Therefore the effective hydrodynamic radius decreases with increasing ionic strength. This reduces the effective headgroup area,  $A_h$  and augments the surfactant packing parameter  $N_s$ . At sufficiently high salt concentration the packing parameter may become  $N_s \sim 1$ , as before bending, so one can anticipate flattening of the bent LC interface at increasing  $\text{NaCl}$  concentration. Exactly that was seen during this test, as shown in Figure 6, where the initially bright texture with Maltese cross became completely dark at about  $250 \mu\text{M}$   $\text{NaCl}$  concentration. This effect therefore supports our qualitative model.

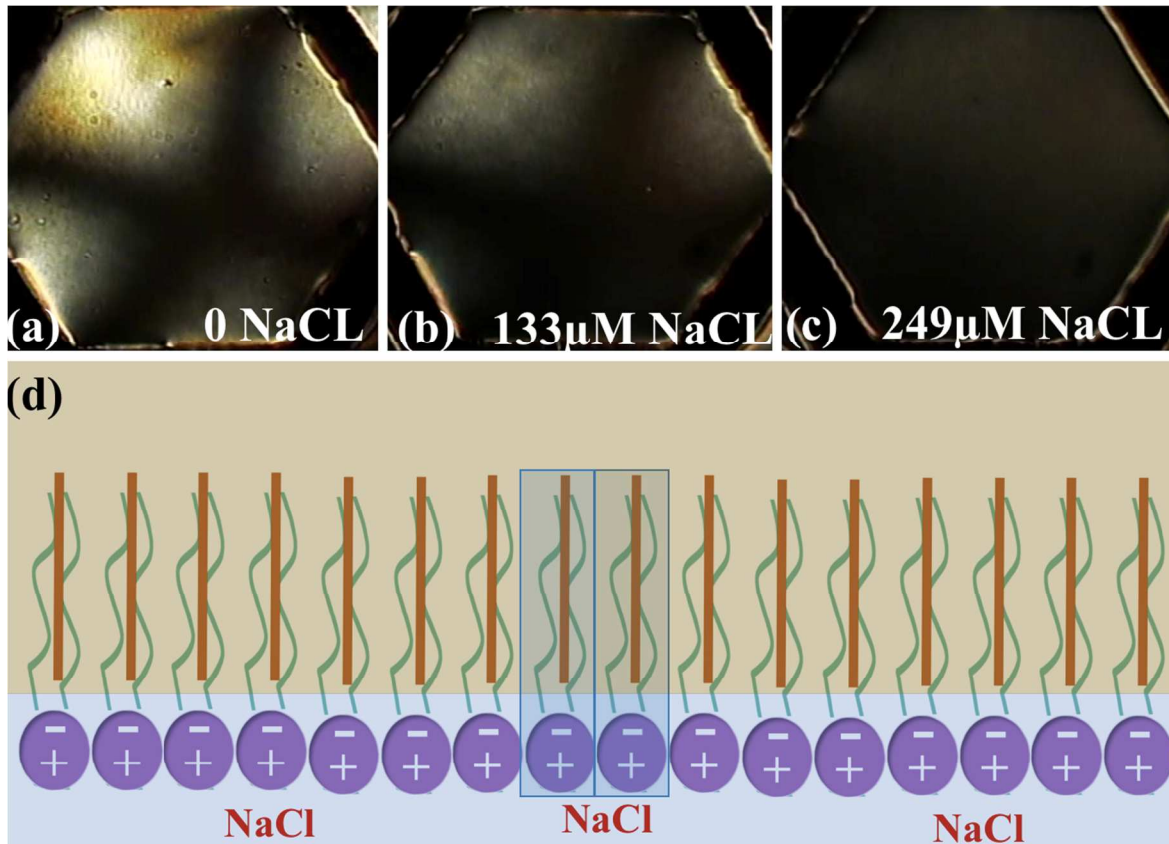


Figure 6: Illustration of the effect of added salt ( $\text{NaCl}$ ) on the texture of the LC film at  $40 \mu\text{M}$  DLPC concentration. (a) No  $\text{NaCl}$  added (texture is the same as shown in Figure 2(c)); (b) The texture at  $133 \mu\text{M}$   $\text{NaCl}$  concentration is darker, though the Maltese cross is still visible, indicating a less bent LC surface; (c) The texture at  $249 \mu\text{M}$   $\text{NaCl}$  concentration is completely dark indicating flat LC film surface with homeotropic alignment; (d) Cartoon of the effect of the  $\text{Na}^+$  and  $\text{Cl}^-$  ions on the effective of the DLPC molecules.

## Summary

In this paper we have investigated the shape of nematic liquid crystal films suspended in sub-millimeter size grids between air and glycerol interfaces when 1,2-dilauroyl-sn-glycero-3-phosphocholine (DLPC) phospholipid was added to glycerol in various (0-100 $\mu$ M) concentrations. Our experiments using an optical profiler revealed that the liquid crystal interface became gradually bent toward the glycerol surface at increasing DLPC concentrations above 1 $\mu$ M. This bending could be reversed by adding NaCl salt to the glycerol/DLPC solution, indicating the role of the packing of the zwitterionic DLPC molecules, which have a reduced effective head group size on addition of the salt. We also demonstrated, within a critical range of lipid concentration where the bending occurs, that the bent interface exhibits extreme sensitivity to air pressure variations, producing an optical response with acoustic stimulation. The reasonable qualitative model we proposed here could explain the main features of these surprising results.

## Acknowledgement:

The work was supported in parts by NSF DMR-0907055, 1506018 and NSF IRES OISE 1259419. A.J. and E.M. acknowledge useful discussions about the model with Prof. Jan Lagerwall and Prof. Edgar Kooijman. We thank to Drs. Attila Nagy and Aladár Czitrovsky for providing the Zygo Profiler for our use and discussing principles of the instrument with us.

## References

- 1 N. A. Lockwood, J. J. de Pablo and N. L. Abbott, *Langmuir*, 2005, **21**, 6805–6814.
- 2 J. M. Brake, A. D. Mezera and N. L. Abbott, *Langmuir*, 2003, **19**, 6436–6442.
- 3 M. Sadati, H. Ramezani-Dakhel, W. Bu, E. Sevgen, Z. Liang, C. Erol, M. Rahimi, N. Taheri Qazvini, B. Lin, N. L. Abbott, B. Roux, M. L. Schlossman and J. J. de Pablo, *J. Am. Chem. Soc.*, 2017, jacs.7b00167.
- 4 P. Popov, D. J. Lacks, A. Jákli and E. K. Mann, *J. Chem. Phys.*, 2014, **141**, 054901.
- 5 A. Pizzirusso, R. Berardi, L. Muccioli, M. Ricci and C. Zannoni, *Chem. Sci.*, 2012, **3**, 573–579.
- 6 H. Ramezani-Dakhel, M. Sadati, M. Rahimi, A. Ramirez-Hernandez, B. B. Roux and J. J. de Pablo, *J. Chem. Theory Comput.*, **13**.

- 7 V. K. Gupta, J. J. J. Skaife, T. B. T. B. Dubrovsky and N. L. L. N. L. Abbott, *Science (80-. )*, 1998, **279**, 2077–2080.
- 8 N. Lockwood and N. Abbott, *Curr. Opin. Colloid Interface Sci.*, 2005, **10**, 111–120.
- 9 Y. Bai and N. L. Abbott, *Langmuir*, 2011, **27**, 5719–5738.
- 10 A. M. Lowe and N. L. Abbott, *Chem. Mater.*, 2012, **24**, 746–758.
- 11 R. J. Carlton, J. T. Hunter, D. S. Miller, R. Abbasi, P. C. Mushenheim, L. N. Tan and N. L. Abbott, *Liq. Cryst. Rev.*, 2013, **1**, 29–51.
- 12 S. Setia, S. Sidiq, J. De, I. Pani and S. K. Pal, *Liq. Cryst.*, 2016, **43**, 2009–2050.
- 13 S. Sidiq and S. K. Pal, *Proc. Indian Natl. Sci. Acad.*, 2016, **82**, 75–98.
- 14 S. Munir, I.-K. Kang and S.-Y. Park, *TrAC Trends Anal. Chem.*, 2016, **83**, 80–94.
- 15 Z. Hussain, F. Qazi, M. I. Ahmed, A. Usman, A. Riaz and A. D. Abbasi, *Biosens. Bioelectron.*, 2016, **85**, 110–127.
- 16 P. Popov, E. K. Mann and A. Jákli, *J. Mater. Chem. B*, 2017, **5**, 5061–5078.
- 17 N. Lockwood, J. Gupta and N. Abbott, *Surf. Sci. Rep.*, 2008, **63**, 255–293.
- 18 L. N. Tan and N. L. Abbott, *J. Colloid Interface Sci.*, 2015, **449**, 452–61.
- 19 S. Yang, C. Wu, H. Tan, Y. Wu, S. Liao, Z. Wu, G. Shen and R. Yu, *Anal. Chem.*, 2013, **85**, 14–18.
- 20 W. Iglesias, N. L. Abbott, E. K. Mann and A. Jákli, *ACS Appl. Mater. Interfaces*, 2012, **4**, 6884–6890.
- 21 P. Popov, L. W. Honaker, E. E. Kooijman, E. K. Mann and A. I. Jákli, *Sens. Biosensing Res.*, 2015, **8**, 31–35.
- 22 P. Popov, E. K. Mann and A. Jákli, *Phys. Rev. Appl.*, 2014, **1**, 034003.
- 23 A. Jakli and A. Saupe, *One- and Two- Dimensional Fluids: Properties of Smectic, Lamellar and Columnar Liquid Crystals*, Taylor and Francis, Boca Raton, 1st edn., 6AD.
- 24 X. Shi, J. Liang and E. Burnett, *J. Archit. Eng.*, 2006, **12**, 93.
- 25 P. Popov, L. W. Honaker, M. Mirheydari, E. K. Mann and A. Jákli, *Sci. Rep.*, 2017, **7**, 1–21.
- 26 F. M. Fowkes, *J. Phys. Chem.*, 1962, **66**, 382–382.
- 27 D. Marsh, *CRC Handbook of Lipid Bilayers*, CRC Press, Boca Raton, Fla, 2nd edn., 2012.
- 28 A. Sorrenti, O. Illa and R. M. Ortuño, *Chem. Soc. Rev.*, 2013, **42**, 8200.
- 29 G. D’Errico, D. Ciccarelli and O. Ortona, *J. Colloid Interface Sci.*, 2005, **286**, 747–754.
- 30 R. Lipowsky and U. Seifert, *Mol. Cryst. Liq. Cryst*, 1991, **202**, 17–25.
- 31 N. Kučerka, Y. Liu, N. Chu, H. I. Petrache, S. Tristram-Nagle and J. F. Nagle, *Biophys. J.*,

- 2005, **88**, 2626–2637.
- 32 J. N. Israelachvili, D. J. Mitchell and B. W. Ninham, *J. Chem. Soc. Faraday Trans. 2*, 1976, **72**, 1525.
- 33 V. V Kumar, *Biophysics (Oxf)*, 1991, 444–448.
- 34 S. Bansal and A. Mittal, *J. Membr. Biol.*, 2013, **246**, 557–570.
- 35 D. Lombardo, M. A. Kiselev, S. Magazù and P. Calandra, *Adv. Condens. Matter Phys.*, 2015, **2015**.
- 36 N. Kučerka, M. P. Nieh and J. Katsaras, *Biochim. Biophys. Acta - Biomembr.*, 2011, **1808**, 2761–2771.

**TOC entry:**

Liquid crystal films suspended between air and glycerol become bent toward the glycerol surface at increasing DLPC concentrations above  $1\mu\text{M}$ .

